



ELSEVIER

Contents lists available at ScienceDirect

Applied Mathematics and Computation

journal homepage: www.elsevier.com/locate/amc

Two-phase flow modeling for low concentration spherical particle motion through a Newtonian fluid

G.J.F. Smit*, J.M. Wilms, G.P.J. Diedericks¹*Department of Applied Mathematics, University of Stellenbosch, Private Bag X1, 7602 Matieland, South Africa*

ARTICLE INFO

Keywords:Two-phase flow
Fluid–solid drag
Closure modeling

ABSTRACT

Models that are used for the simulation of two-phase flows in coastal dynamics make extensive use of empirical data. The main focus of this investigation is to develop models for specific aspects of two-phase flows that are based on physical principles in order to reduce the use of such data. In this study several existing empirically based drag force models are discussed. The motion of spherical or near-spherical solid particles through a Newtonian fluid is investigated and a new method for closure of the drag force, using a Representative Unit Cell is discussed and compared to the existing models as well as to experimental data. The various drag models were also evaluated by numerical simulations, using an in-house developed program based on an adaptation of the SIMPLE procedure.

© 2010 Elsevier Inc. All rights reserved.

1. Introduction

The theoretical analysis and numerical modeling of multiphase flow has increasingly become the subject of considerable attention in engineering and several life and earth sciences. This type of flow frequently occurs naturally, such as the flow of blood, fluidized beds, transport of pollutants in aquifers, solute transport in reactors in the chemical industry and sediment transport. According to Hassan and Ribberink [1], accurate sediment transport models are essential to simulate and predict large-scale and long term morphological changes in the coastal zone. The main objective of this study is to put forward a formalism in which the movement of suspended sediments can be treated as two-phase flow, built on the concept of volume averaging. The model verification presented in this study is for the simplified case of vertical settling of particles.

The theoretical basis for studying of such two-phase processes must be formulated in terms of the unsteady motion of various phases having unequal velocities and temperatures, coupled through drag, mass and energy transfer. Various different modeling strategies are used, which may broadly be categorized into two types of approaches, namely trajectory models, where the dispersed particle phase is evaluated by either tracing single particles or a cloud of particles, and fluid models which treat the phases as continuous media. Some examples of fluid models include homogeneous-flow models, drift-flux models and two-fluid models.

The homogeneous-flow model treats the two phases as a single homogeneous fluid. The equations are therefore the same as those for (single-phase) homogeneous flow modeling. This method of modeling, although relatively easy to use, is limiting in the sense that it cannot model the transfer, i.e. of mass, momentum and energy, between phases. In drift-flux models the phases are separated in terms of the relative motion of the different phases. It describes the effects of the velocity differences in terms of the drift velocity, i.e. the difference between the phase velocity and the total volumetric flux. Although the drift-flux model expresses the velocity differences it does not take into account the phase and velocity distributions.

* Corresponding author.

E-mail address: fsmit@sun.ac.za (G.J.F. Smit).¹ CSIR, Natural Resources and the Environment, P.O. Box 320, Stellenbosch 7599, South Africa.

For the two-fluid models a full set of conservation equations is solved for each of the two phases simultaneously, along with constitutive equations describing the inter-phase coupling. To bypass the necessity to model the discrete nature of separate phases at the microscopic level, averaging (of time, volume and/or mass) methods are used, thereby transforming the problem to a macroscopic level.

Whitaker [2], Slattery [3], and Bachmat and Bear [4], were amongst the pioneers in the development of the technique of local volume averaging. According to the volume averaging procedure, interstitial (or microscopic) transport entities and equations may be averaged volumetrically over a representative elementary volume to derive macroscopic balance equations for various transport phenomena. In the derivation of the averaged equations Zhang and Prosperetti [5], averaged the particle momentum equation directly rather than the momentum equation of the particle material. The additional terms that originated from these derivations contain the inter-phase momentum transfer.

The medium considered in this study consists of two phases, a (single) fluid phase and a solid phase consisting of solid particles such as cohesionless sediment particles moving in a water column. The principles of modeling flow through isotropic granular porous media, using volumetric averaging procedures, are adapted and extended to the modeling of two-phase flow.

2. Two-phase flow model

2.1. Momentum equations

For the volumetric averaging of the transport equations, describing the flow, the concept of a Representative Elementary Volume (REV) is often used. An REV is defined as a control volume that always, independent of its location within the porous medium, comprises of both phases in the correct locally average proportions. (For further details regarding the selection of a suitable REV the reader is referred to, e.g., Whitaker [2], Hassanizadeh and Gray [6], Bachmat and Bear [4], and Bear and Bachmat [7].)

Assume that ϕ is some extensive (a volumetric additive) quantity of the fluid phase, which is assumed to be finite, continuous and differentiable within an REV, with volume U_o . Also assume that the fluid phase is multiply-connected, i.e. any two points within the phase can be connected by a continuous curve that lies completely within it. The intrinsic phase average of the quantity ϕ of the fluid phase within an REV is then defined by

$$\phi_f = \frac{1}{U_f} \int \int_{U_f} \phi dU_f, \quad (1)$$

where U_f is the volume fluid phase within the REV. Applying volume averaging, over an REV, to the time dependent fluid phase momentum equation, ignoring all deviation terms and assuming that the fluid density is constant, yields:

$$\rho_f \frac{\partial}{\partial t} (\varepsilon \underline{v}_f) + \rho_f \nabla \cdot (\varepsilon \underline{v}_f \underline{v}_f) = \varepsilon \rho_f \underline{g} - \varepsilon \nabla p_f + \mu \nabla \cdot (\varepsilon \nabla \underline{v}_f) - \underline{E}_{Drag}, \quad (2)$$

where the drag force term is

$$\underline{E}_{Drag} = \beta (\underline{v}_f - \underline{v}_s) \quad (3)$$

with β the momentum transfer coefficient. In Eqs. (2) and (3), ρ_f is the fluid density, $\varepsilon (=U_f/U_o)$ the fluid volume fraction, g the gravitational constant, μ the fluid viscosity, p_f the average fluid pressure, and \underline{v}_f and \underline{v}_s the average fluid and solid velocities.

It is assumed that the solid phase consists of discrete solid deformable particles which are (almost) completely surrounded by the fluid. Thus the solid phase is composed of an union of disjoint domains, with disjoint boundaries and because it is non-connected, additional averaging procedures (than those used for the continuous fluid phase) have to be used. Therefore, define an intrinsic volumetric average of an extensive quantity of a number n of discrete particles as follows:

$$\gamma_s \equiv \frac{1}{U_s} \sum_{i=1}^n \gamma_i U_i, \quad (4)$$

where

$U_s \equiv$ the total volume of all the solid particles in the REV,

$U_i \equiv$ the volume of particle i ,

$\gamma_i \equiv$ extensive quantity of particle i defined at the centroid of the particle.

From the above definition it is assumed that γ_i either prevails over the whole particle or that γ_i is an average of the quantity γ defined at the centroid of the particle. The above formulation can also be considered as the volume weighted value of γ .

The change in momentum of a single solid particle i can be described as:

$$m_i \frac{d\underline{v}_i}{dt} = m_i \underline{g} + \sum E, \quad (5)$$

where m_i is the mass of particle i , \underline{v}_i its velocity and the last term in Eq. (5) represents all external forces apart from gravity. Summation of Eq. (5) over all particles in an REV and applying Eq. (4), the solid phase momentum can be written as:

$$\rho_s \frac{\partial}{\partial t} (\varepsilon_s \underline{v}_s) + \rho_s \nabla \cdot (\varepsilon_s \underline{v}_s \underline{v}_s) = \varepsilon_s (\rho_s - \rho_f) \underline{g} + \beta (\underline{v}_f - \underline{v}_s) + \sum F_{Other}, \quad (6)$$

where ρ_s is the solid density and $\varepsilon_s (=1 - \varepsilon)$ is the solid volume fraction. The term F_{Other} in Eq. (6) describes all forces other than buoyancy and drag, e.g. Saffman forces, particle–particle interaction, etc. For the remainder of this paper we will ignore the latter forces described by the last term in Eq. (6).

The drag force term, Eq. (3), provides the coupling between the momentum equations of the two respective phases, i.e. Eqs. (2) and (6).

2.2. Drag forces in fluid–solid flows

2.2.1. Ergun

The momentum transfer coefficient described by the well known and frequently used Ergun equation is:

$$\beta = \frac{150 \mu \varepsilon_s^2}{d_s^2 \varepsilon^2} + \frac{1.75 \rho_f \varepsilon_s \|\underline{v}_f - \underline{v}_s\|}{d_s \varepsilon}, \quad (7)$$

where d_s is the diameter of a solid particle.

The Ergun equation, however, was developed for packed beds and does not account for large variations in concentration as is found in sedimentation problems. In spite of this limitation, it is commonly employed by many researchers over a wide range of bed void fractions. It is used in the multiphase flow model, proposed by Gidaspow [8] which is adopted as default in the majority of commercial CFD codes used to date (e.g. Fluent). This correlation is used for values of the fluid volume fraction up to 0.80.

2.2.2. Lewis, Wen and Yu and Kmic

Typical models of drag force in uniformly dispersed emulsions of solid particles are those based on the work by Kmic [9], Lewis et al. [10], and Wen and Yu [11]:

$$\beta = \frac{3}{4} C_D(\text{Re}) \frac{\rho_f \|\underline{v}_f - \underline{v}_s\| (1 - \varepsilon)}{d_s} \varepsilon^{-\alpha}, \quad (8)$$

where C_D is the drag coefficient that is a function of the Reynolds number. The Reynolds number is given by

$$\text{Re} = \frac{\rho_f \varepsilon d_s}{\mu} \|\underline{v}_f - \underline{v}_s\|, \quad (9)$$

and $\alpha = 2.65$ [10]; $\alpha = 2.70$ [11]; $\alpha = 2.78$ [9].

The equation developed by Lewis et al. [10] is usually adopted as a default correlation in commercial CFD codes when the void fraction of the suspension exceeds the threshold value of 0.80 [12]. In Eq. (8) the drag coefficient is:

$$C_D(\text{Re}) = \begin{cases} \frac{24}{\text{Re}} (1 + 0.15 \text{Re}^{0.687}) & \text{for } \text{Re} < 1000 \\ 0.44 & \text{for } \text{Re} \geq 1000 \end{cases}. \quad (10)$$

The drag coefficient described by Eq. (10) consists of the drag coefficient for two limiting flow regimes, i.e. $C_D \rightarrow 24/\text{Re}$ for very low Reynolds numbers and $C_D \rightarrow 0.44$ at high Reynolds numbers. An asymptotic matching technique described by Churchill and Usagi [17] may be used to produce a combined result which is valid for both of these ranges. Therefore, for comparison purposes (for this study), the drag coefficient may be written as:

$$C_D(\text{Re}) = \left(\left(\frac{24}{\text{Re}} \right)^s + 0.44^s \right)^{1/s}, \quad (11)$$

where the shifting parameter, s , determines the extent of overlap between the two physical conditions describing the two limiting expressions. In Fig. 1 the drag coefficients described by Eqs. (10) and (11) are compared as functions of Reynolds number. Two values of the shifting parameter s , namely $s = 1.0$ and $s = 0.5$, were used in Eq. (11).

2.3. Representative unit cell model

The drag force on the solid particles in two-phase flow can be inferred from the drag on stationary solid particles typically encountered in flow through porous media. Applying the volumetric phase averaging procedure to the continuous fluid momentum equation for flow through a stationary porous medium, and assuming uniform average flow through a stationary porous medium of uniform porosity, the pressure gradient is [16]

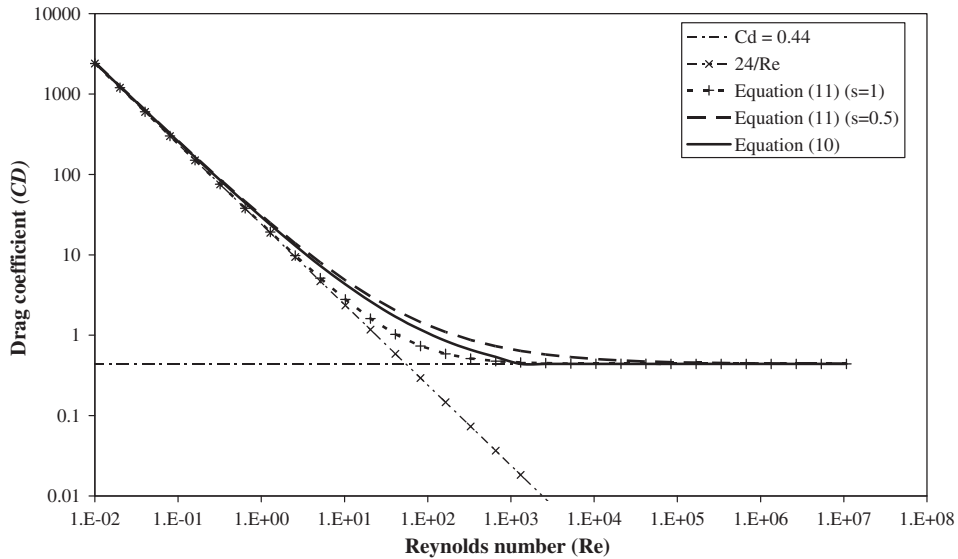


Fig. 1. Drag coefficient as a function of Reynolds number.

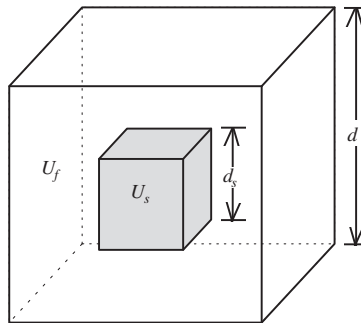


Fig. 2. Representative Unit Cell (RUC).

$$-\varepsilon \nabla p_f = \frac{1}{U_o} \int \int_{S_{fs}} (\underline{n} p - \underline{n} \cdot \underline{\tau}) dS. \tag{12}$$

In Eq. (12) p_f is the average fluid pressure, S_{fs} the fluid–solid interface, \underline{n} is a normal vector on the fluid–solid interface pointing in the direction of the solid and $\underline{\tau}$ is the stress dyad.

This equation is “open” in the sense that the variables are still undetermined and the equation is valid for any porous medium microstructure. Secondary modeling is therefore needed to transform Eq. (12) into a closed form for a particular application which can then be solved analytically or numerically.

Different approaches for the secondary averaging exist, but in this case the interstitial flow is analyzed on a microscopic scale by means of a Representative Unit Cell (RUC) [13,14]. For a granular porous medium the average geometrical properties of the solid structure within the RUC may be resembled by a cube of solid material as shown in Fig. 2. A two-dimensional schematic of the RUC is shown in Fig. 3. The RUC has a volume of U_o and linear dimension, d . The width and volume of the solid is respectively given by d_s and U_s . The fluid volume is denoted by U_f and is divided into stream-wise, $U_{||}$, and transverse, U_{\perp} , sections. The fluid–solid interface, S_{fs} , is divided into its stream-wise, $S_{||}$, and transverse, S_{\perp} , sections. The outward directed unit vectors for the fluid and solid phases are depicted by \underline{n}_f and \underline{n}_s respectively. The description of the RUC was done in detail in Du Plessis and Diedericks [15], and therefore will not be repeated here.

Eq. (12) can be generalized to account for both the low Reynolds number flow, i.e. Darcy regime where only viscous drag is present, and the Forchheimer regime of higher Reynolds number (but still laminar) flow.

In the Darcy flow regime, the frictional forces on the fluid–solid interfaces, as captured in the fluid–solid integral term in Eq. (12), are the primary causes for pressure losses through the porous medium. The pressure loss is a direct result of the wall shear stresses. Taking into consideration stream-wise, transverse, transfer and stagnant volumes and surfaces [16] for

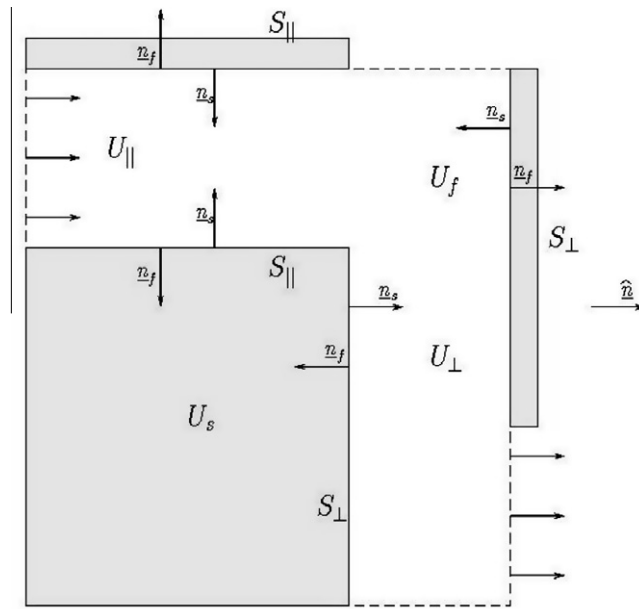


Fig. 3. Two dimensional RUC.

various staggering configurations, the one-dimensional form of the gradient of the intrinsic phase average pressure for purely viscous creep flow may then be expressed as

$$\varepsilon \frac{dp_f}{dx} = \beta_0 v_f = \left[\frac{25.4 \mu \varepsilon^2 (1 - \varepsilon)^{4/3}}{d_s^2 (1 - (1 - \varepsilon)^{2/3})^2 (1 - (1 - \varepsilon)^{1/3})} \right] v_f. \quad (13)$$

In Eq. (13) v_f represents the average of speed of the fluid, and β_0 is the momentum drag coefficient in the Darcy flow regime.

In the intermediate Reynolds number flow regime, albeit still within the laminar range, it is assumed that flow re-circulation is developed but no turbulence is yet present and form drag is assumed [15] yielding:

$$\varepsilon \frac{dp_f}{dx} = \beta_\infty v_f = \left[\frac{C_D \rho_f \varepsilon^2 (1 - \varepsilon)}{2d_s (1 - (1 - \varepsilon)^{2/3})^2 \|u_f\|} \right] v_f, \quad (14)$$

where for the RUC model C_D is considered as a form drag coefficient and β_∞ is the momentum transfer coefficient for the Forchheimer flow regime.

Since each two of the above limiting expressions predominates in their respective regions of applicability, an unified model can be obtained using an asymptote matching technique [17]. Therefore combining Eqs. (13) and (14) results in a general expression for predicting the pressure gradient of purely viscous flow through a granular porous medium, yielding

$$\varepsilon \frac{dp_f}{dx} = \beta v_f = [\beta_0^s + \beta_\infty^s]^{1/s} v_f = \left[\left(\frac{25.4 \mu \varepsilon^2 (1 - \varepsilon)^{4/3}}{d_s^2 (1 - (1 - \varepsilon)^{2/3})^2 (1 - (1 - \varepsilon)^{1/3})} \right)^s + \left(\frac{C_D \rho_f \varepsilon^2 (1 - \varepsilon)}{2d_s (1 - (1 - \varepsilon)^{2/3})^2 \|u_f\|} \right)^s \right]^{1/s} v_f. \quad (15)$$

For flow through a stationary porous medium and with relatively low porosity ($\varepsilon \approx 0.43$), the values of $s = 1$ and $C_D = 1.95$ were found to give good results when comparing to results from the Ergun equation [16].

Eq. (15) provides an expression for the forces between the fluid phase and stationary porous medium, consisting of solid particles. By introducing the relative velocity between the two phases, the RUC model for flow through a stationary porous medium can be adapted to be applicable to two-phase flow, resulting in the following expression for the drag force coefficient:

$$\beta = \left[\left(\frac{25.4 \mu \varepsilon^2 (1 - \varepsilon)^{4/3}}{d_s^2 (1 - (1 - \varepsilon)^{1/3}) (1 - (1 - \varepsilon)^{2/3})^2} \right)^s + \left(\frac{C_D \rho_f \varepsilon^2 (1 - \varepsilon)}{2d_s (1 - (1 - \varepsilon)^{2/3})^2 \|u_f - u_s\|} \right)^s \right]^{1/s}. \quad (16)$$

However, for very low Reynolds numbers and ε close to unity, drag must represent Stokes drag for a single particle, i.e. $C_D \rightarrow 24/Re$, which means that

$$\beta \rightarrow \frac{18\mu(1-\varepsilon)}{d_s^2}. \quad (17)$$

Furthermore for high Reynolds number flows and ε close to unity, C_D should be 0.44, as for a single particle.

Following the results presented in Fig. 1 (of Eq. (11)), it was found that the shifting parameter $s = 0.5$ gives good results for very low solid volume fraction (compared to the 1 for relatively high solid volume fraction). The drag force coefficient, based on the RUC model, for very low solid concentration can then be written as:

$$\beta_{RUC} = \left[\left\{ \frac{\mu(1-\varepsilon)}{d_s^2} \left(\frac{25.4\varepsilon^2(1-\varepsilon)^{1/3}}{(1-(1-\varepsilon)^{1/3})(1-(1-\varepsilon)^{2/3})^2} + 18 \right) \right\}^{0.5} + \left\{ \frac{0.44\rho_f\varepsilon^2(1-\varepsilon)}{2d_s(1-(1-\varepsilon)^{2/3})} \|\underline{v}_f - \underline{v}_s\| \right\}^{0.57} \right]^2. \quad (18)$$

3. Model evaluation

In the simplified case of vertical setting of particles, from Eq. (6) the terminal speed of the solid particles may be determined by:

$$-\varepsilon_s(\rho_s - \rho_f)g = \beta(v_f - v_s). \quad (19)$$

The proposed RUC model was evaluated, experimentally and numerically, by evaluating the terminal speed of particles falling under gravity through fresh water and comparing it to predicted results using Eq. (19).

3.1. Experimental

A settling or fall tube, shown in Fig. 4, was used to determine the terminal speeds with which particles settle through the water column. The following procedure was followed [18]: A sample of particles is spread evenly onto the insertion plate in a layer of approximately one grain thickness. The plate and the sample are moistened with water to ensure adhesion of the particles to the plate. The insertion plate and sample are inverted and placed into the cradle/collar at the top of the tube. The cradle is lowered smoothly by rotation until the insertion plate and sample make contact with the water. The moment the sample touches the water, the adhesive forces are broken and the particles start to fall. Simultaneously, the dip switch triggers the timer.

After falling the length of the tube, the particles land on the weighing pan and the strain gauge registers the increasing strain due to the accumulation of the particles on the pan. The strain is captured and provides an instantaneous readout of the sample accumulation. An example result is shown in Fig. 5 where the increasing strain is shown as a function of time after insertion.

Additionally, a camera was placed adjacent to the settling tube and the falling particles were photographed at 30 fps. The positions of a representative (in terms of speed distribution) portion of the particles were digitized relative to the axis system, and the speeds of the particles were calculated. The test set-up and example of particles photographed are shown in



Fig. 4. Settling tube.

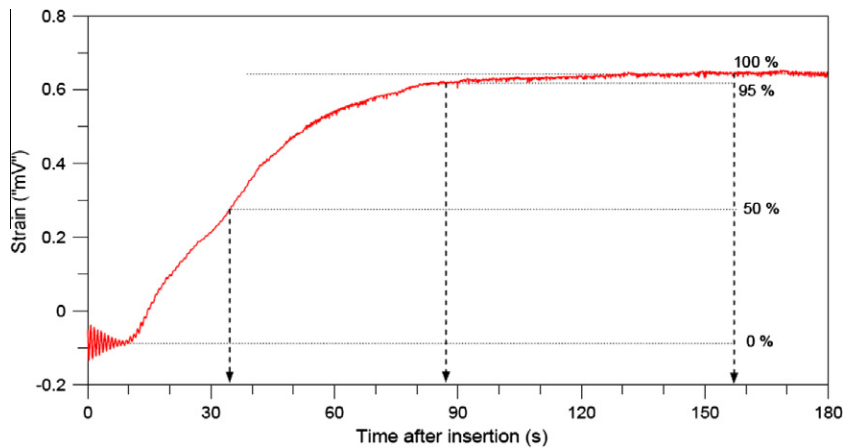


Fig. 5. Sample output from settling tube [18].

Fig. 6 From the figure it can be seen that the particles tend to be dispersed, and therefore particles were tracked in three zones, representing faster, average and slower speeds.

Spherical glass beads ranging from 0.15 mm to 1.0 mm in diameter, as listed in Table 1, were used in the experiments. The specific weight of the beads was 2.5 g/cm^3 .

3.2. Numerical implementation

The numerical simulations were done with an in-house developed finite volume program. The segregated single-fluid pressure based algorithm, SIMPLE, was extended by deriving the pressure-correction equation from overall mass conservation (the sum of the respective volume fractions is equal to one) i.e.

$$\nabla \cdot (\varepsilon_f \mathbf{v}_f + \varepsilon_s \mathbf{v}_s) = 0.$$

The mass conservation equations of the solid and fluid phases were solved after a converged solution was obtained for the velocity fields of both phases, and the pressure field. This algorithm forms part of the Mass Conservation Based Algorithms (MCBA) as described by Darwish et al. [19]. Upwind differencing of the convective terms was used and interface coupling was done through the drag term, based on the RUC drag equation. Fig. 7 is the visualization of the output of from the numerical program. The figure shows the concentration of the particles at three different positions, illustrating the particles falling through the water at terminal speed.

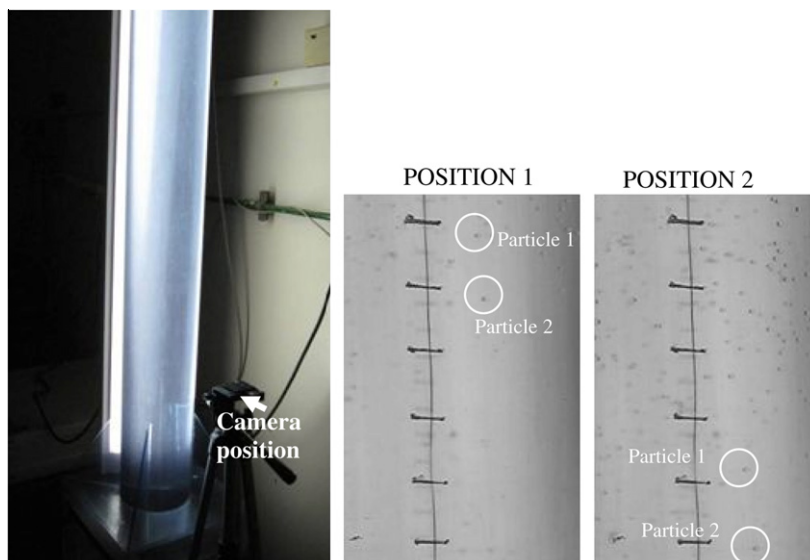


Fig. 6. Camera position and sample photographs.

Table 1
Particle sizes.

Size Range (mm)	Average (mm)
0.15–0.25	0.2
0.20–0.30	0.25
0.25–0.50	0.375
0.50–0.75	0.625
0.75–1.00	0.875

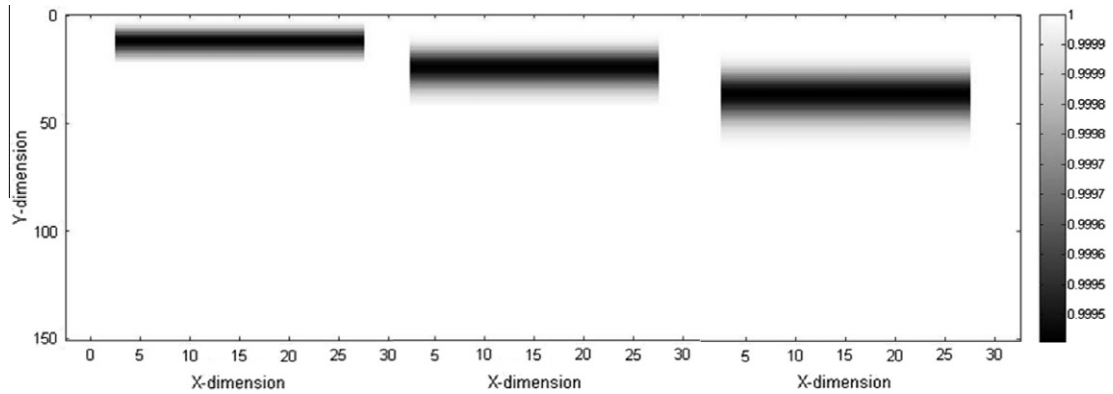


Fig. 7. Visualization of output from numerical simulation.

4. Results and discussion

For relatively high solid concentration flows, i.e. for fluid void fractions of $\varepsilon \sim 0.43$, the RUC model compares favorably with the Ergun equation, as illustrated in Fig. 8. As expected, the model of Lewis et al. [10], over-predicts the momentum transfer coefficient as the particular void fraction falls outside the model's range of applicability.

Fig. 9 shows that the predicted momentum transfer coefficient of the RUC model for very low solid concentration, i.e. for fluid void fractions of $\varepsilon \sim 0.9996$, is in good agreement with the results from Lewis et al. [10].

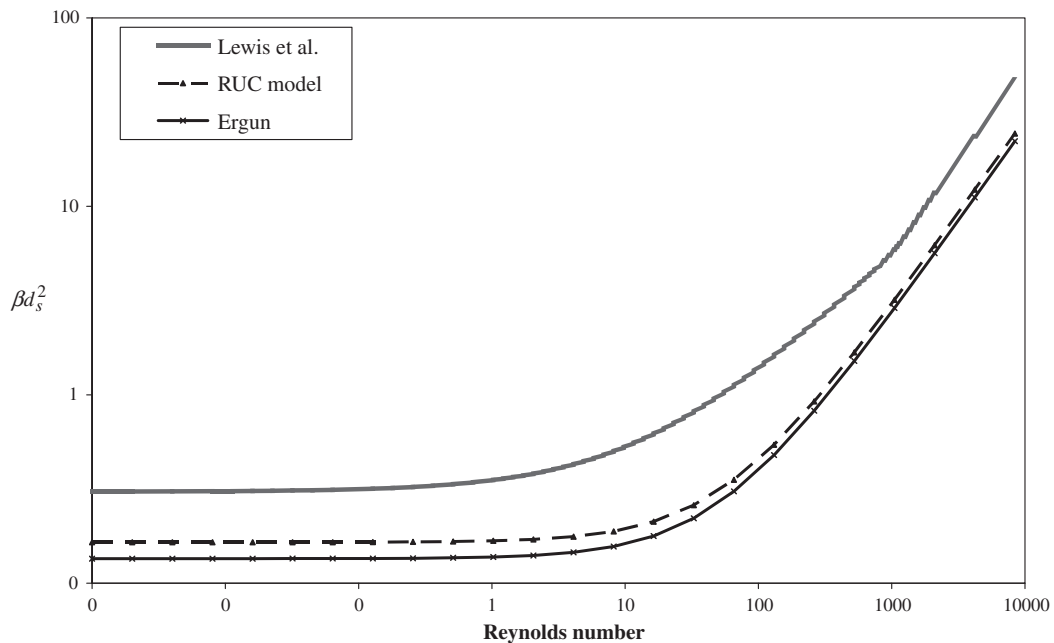


Fig. 8. Comparison between proposed model and Ergun : $s = 1.0$, $\varepsilon = 0.43$, $C_D = 1.95$.

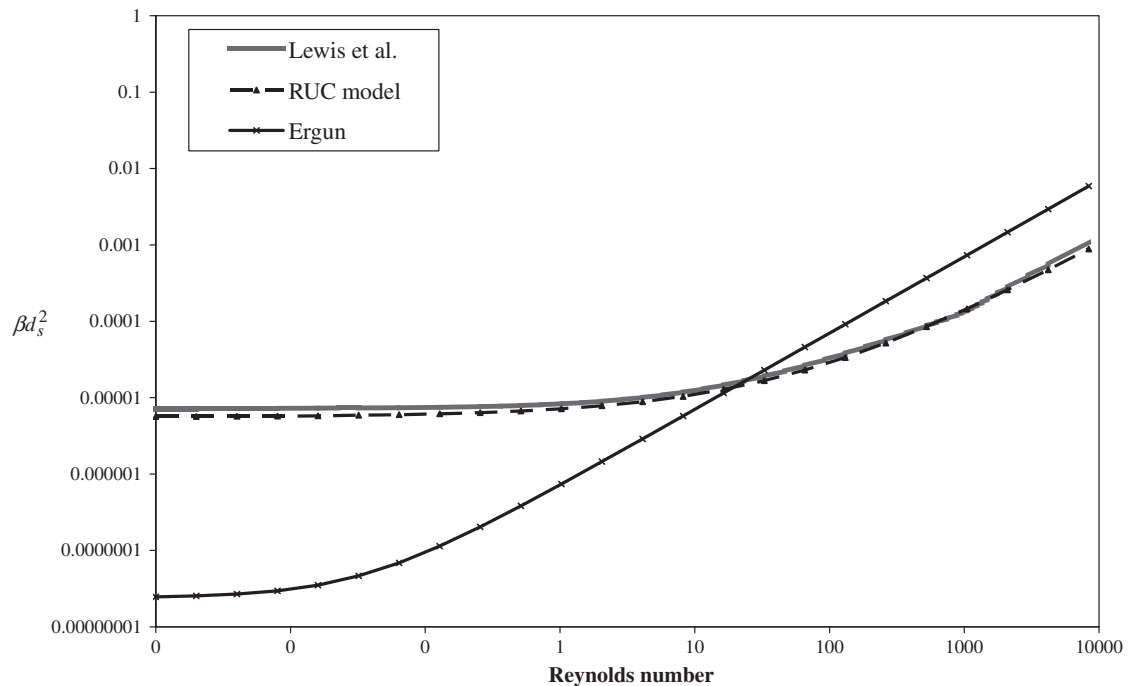


Fig. 9. Comparison between proposed model and Lewis et al. : $s = 0.5$, $\varepsilon = 0.9996$, $C_D = 0.44$.

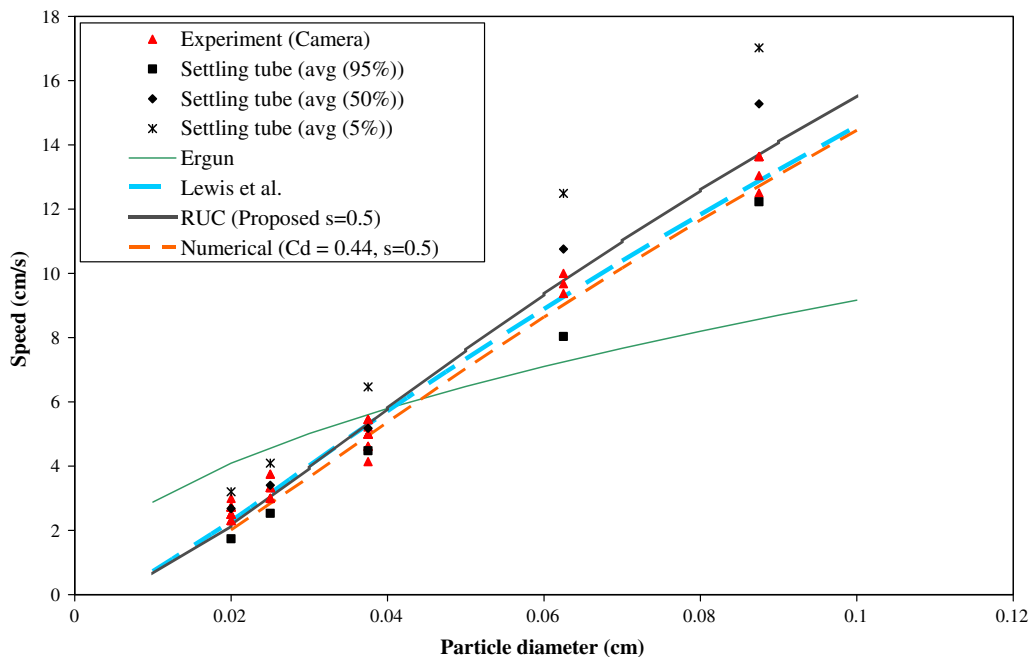


Fig. 10. Analytical and numerical results compared to experimental data.

In Fig. 10 the predicted (analytically and numerically) settling speeds are compared to the experimentally determined speeds, as obtained from the settling tube data as well as the digitized data from the photographs. The 5, 50 and 95% values for the settling tube refer to the average speeds of the respective percentages of particles that have settled on the weighing pan. The three speed values shown for the camera data represent the speeds of particles near the bottom of the tube tracked in three zones of the dispersed cloud. Therefore, these show less variation than the settling tube data. The numerically and

analytically predicted data, based on the RUC model, are in agreement with each other. The value of this result is that the in-house developed computer program performs correctly in the limit of vertically falling particles. In addition, both the numerically and analytically predicted data compare favorably with the test results.

5. Conclusion

A new closure relationship for the drag force has been proposed for systems of dispersed particles of spherical shape. The proposed model is valid for high to low solid volume fractions over a wide range of Reynolds numbers. For low solid volume fractions a good correlation is seen with experimental data and other empirical relations.

The value of the shifting parameter s used in Eq. (17) is a function of the solid volume fraction, ranging from unity for relatively high volume fractions to in the order of 0.5 for the low volume fractions. Quantifying the parameter, s , in terms of the volume fraction, forms part of ongoing research.

The additional forces referred to in Eq. (6) and their relative importance to the drag term is currently being investigated. Since this work has only been tested experimentally for low solid volume fraction cases, special attention is given to the influence that particle–particle interactions will have on higher concentration scenarios. Establishing the dependence of s on physical parameters will provide deeper insight into the underlying physics governing multi-phase flow and the ideal would be an expression which consists entirely of measurable physical parameters.

Acknowledgements

The following institutions and people are acknowledged: The National research foundation of South Africa for financial assistance and the CSIR and Christoph Soltau for assistance with the experimental setup.

References

- [1] W.N.M. Hassan, J.S. Ribberink, Modelling of sand transport under wave-generated sheet flow with a RANS diffusion model, *Coastal Engineering* 57 (2010) 19–29.
- [2] S. Whitaker, Diffusion and dispersion in porous media, *AIChE Journal* 13 (1967) 420–427.
- [3] J.C. Slattery, Single phase flow through porous media, *AIChE Journal* 15 (1969) 866–872.
- [4] Y. Bachmat, Macroscopic modeling of transport phenomena in porous media, 1: the continuum approach, *Transport in Porous Media* 1 (1986) 213–240.
- [5] D.Z. Zhang, A. Prosperetti, Averaged equations for inviscid disperse two-phase flow, *Journal of Fluid Mechanics* 267 (1994) 185–219.
- [6] M. Hassanizadeh, W.G. Gray, General averaging equations for multi-phase systems: 1 averaging procedure, *Advances in Water Resources* 2 (1979) 131–144.
- [7] J. Bear, Y. Bachmat, *Introduction to Modeling of Transport Phenomena in Porous Media*, Kluwer Academic Publishers, 1991. ISBN 0-7923-1106-X.
- [8] D. Gidaspo, *Multiphase Flow and Fluidization: Continuum and Kinetic Theory Descriptions*, Academic Press, New York, 1994.
- [9] A. Kmiec, Equilibrium of forces in a fluidized bed – experimental verification, *Journal of Chemical Engineering* 23 (1982) 133.
- [10] W.K. Lewis, W.C. Gilliland, W.C. Bauer, Characteristics of fluidized particles, *Industrial and Engineering Chemistry* 41 (1949) 1104.
- [11] C.Y. Wen, Y.H. Yu, *Mechanics of Fluidization*, Chemical Engineering Progress Symposium Series 62 (1966) 100.
- [12] I. Mazzei, P. Lettieri, A drag force closure for uniformly dispersed fluidized suspensions, *Chemical Engineering Science* 62 (2007) 6129–6142.
- [13] J.P. Du Plessis, J.H. Masliyah, Mathematical modelling of flow through consolidated isotropic porous media, *Transport in Porous Media* 3 (1988) 145–161.
- [14] J.P. Du Plessis, J.H. Masliyah, Flow through isotropic granular porous media, *Transport in Porous Media* 6 (1991) 207–221.
- [15] J.P. Du Plessis, G.P.J. Diedericks, Pore-scale modeling of interstitial transport phenomena, Chapter 2, *Fluid transport in Porous Media*, in: J.P. du Plessis (Ed.), *Advances in Fluid Mechanics Series*, C M Publication, Southampton, 1997.
- [16] J.P. Du Plessis, S. Woudberg, Pore-scale derivation of the Ergun equation to enhance its adaptability and generalization, *Chemical Engineering Science* 63 (2008) 2576–2586.
- [17] S.W. Churchill, R. Usagi, A general expression for the correlation of rates of transfer and other phenomena, *AIChE Journal* 18 (6) (1972) 1121–1128.
- [18] C. Soltau, Investigation of the grain sizes of longshore transport zone, MSc Thesis, Stellenbosch University, South Africa, 2009.
- [19] M. Darwish, F. Moukalled, B. Sekar, *Numerical heat transfer* 40 (2001) 99–137.